A Journal of the Gesellschaft Deutscher Chemiker

Angewandte International Edition GDCh Chemie

www.angewandte.org

Accepted Article

Title: Enantiomorphic Microvortex-Enabled Supramolecular Sensing of Racemic Amino Acids using Achiral Building Blocks

Authors: Yike Li, Chao Liu, Xuan Bai, Fei Tian, Guoqing Hu, and Jiashu Sun

To be cited as: *Angew. Chem. Int. Ed.* 10.1002/anie.201913882
Angew. Chem. 10.1002/ange.201913882

Link to VoR: http://dx.doi.org/10.1002/anie.201913882
http://dx.doi.org/10.1002/ange.201913882

WILEY-VCH

10.1002/anie.201913882

WILEY-VCH

Enantiomorphic Microvortex-Enabled Supramolecular Sensing of Racemic Amino Acids using Achiral Building Blocks

Yike Li,[+[a,b]] Chao Liu,[+[a,b]] Xuan Bai,[+[b,d]] Fei Tian,[[a,b]] Guoqing Hu,[[c]] and Jiashu Sun*[[a,b]]

Abstract: Chiral analysis of bioactive molecules is of increasing significance in chemical and life sciences. However, the quantitative detection of a racemic mixture of enantiomers is a challenging task, which currently relies on complicated and time-consuming multiple steps of chiral derivatization, chiral separation, and spectroscopic measurement. Herein, we show that, without the use of any chiral molecules and pretreatment steps, the co-assembly of amino acids with achiral $TPPS_4$ monomers controlled by enantiomorphic microvortices allows for quantitative detection of racemic or enantiomeric amino acids, through analysis of sign and magnitude of supramolecular chirality in different outlets of a microfluidic platform. A simulation model demonstrates that chiral microvortices can induce an initial chiral bias by bending the sheet structure, resulting in supramolecular self-assembly of $TPPS_4$ and amino acids of compatible chirality by the self-sorting. This enantiomorphic microvortex-enabled supramolecular sensing system may find versatile applications in chiral sensing.

Chirality is a fundamental aspect of nature, playing important role in chemical and biological processes such as asymmetric catalysis, protein folding, and DNA duplication.[1] Certain bioactive chiral molecules, i.e. amino acids, occur in both L- and D-forms, but exhibiting significant difference in the physiological activities.[2] Chiral analysis of amino acids is of increasing significance in chemical science, pharmaceutical industry, and other related fields.[3] Circular dichroism (CD) spectroscopy is one of the most widely applicable techniques for determining the absolute configuration of chiral analytes.[4] Despite its growing use, CD spectroscopy is difficult to detect amino acids lacking strong chromophoric groups as well as the racemic mixture of amino acid enantiomers, both of which show weak chiro-optical response.[5]

The assembly of chiral amino acids with achiral building blocks can transfer the chiral information to the supramolecular aggregates through the weak intermolecular interactions. For example, D- and L-amino acids promote the formation of J-aggregates of tetra-(4-sulfonatophenyl) porphyrin ($TPPS_4$) and induce opposite CD signals of the supramolecular assembly.[6] The self-assembly of racemic alanine derivatives leads to formation of supramolecular twisted ribbons, allowing for enantioselective detection of various amino acids based on the chiral interactions.[7] The investigation of self-induced diastereomeric anisochronism effect enables characterization of racemic and enantiopure samples based on their different chemical shifts in nuclear magnetic resonance spectroscopy.[8] In addition, the induction of large chiral hydrodynamic gradients by a stirring vortex can also select the chiral sign of J-aggregates of $TPPS_4$ in the absence of chiral molecules.[9] The coupling of chiral mechanical effect to the supramolecular system may provide a tremendous opportunity to detect the racemic mixture of amino acids.[10]

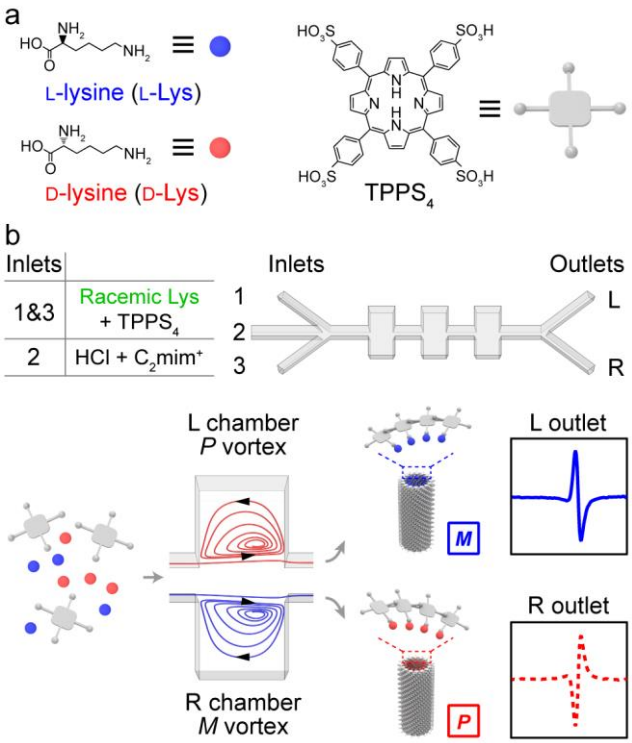

Figure 1. Schematic of enantiomorphic microvortex-enabled detection of racemic Lys by co-assembly with achiral $TPPS_4$ monomers. (a) Chemical structures of L-Lys (blue), D-Lys (red), and $TPPS_4$ (gray). (b) *P* and *M* helical microvortices in the opposite microchambers controlling the co-assembly of $TPPS_4$ and racemic Lys at the initial state, leading to the formation of supramolecular assemblies of *M* and *P* chirality, the sign and intensity of which indicate the presence and concentration of racemic Lys.

[a] Y. Li, Dr. C. Liu, Dr. F. Tian, Prof. J. Sun
CAS Key Laboratory of Standardization and Measurement for Nanotechnology, CAS Center for Excellence in Nanoscience
National Center for Nanoscience and Technology,
Beijing 100190 (China)
E-mail: sunjs@nanoctr.cn
[b] Y. Li, Dr. C. Liu, X. Bai, Dr. F. Tian, Prof. J. Sun
School of Future Technology, University of Chinese Academy of Sciences, Beijing 100149 (China)
[c] Prof. G. Hu
Department of Engineering Mechanics, Zhejiang University, Hangzhou 310027 (China)
[d] X. Bai
The State Key Laboratory of Nonlinear Mechanics, Institute of Mechanics, Chinese Academy of Sciences, Beijing 100190 (China)

[+] These authors contributed equally to this work.
Supporting information for this article is given via a link at the end of the document.

Here, we show that the enantiomorphic microvortex-controlled co-assembly of amino acids with achiral $TPPS_4$ building blocks enables quantitative detection of amino acids in racemic or enantiomeric form. Using a microfluidic platform to generate right-handed (*P*) and left-handed (*M*) helical microvortices in the opposite microchambers, the chirality of initially formed $TPPS_4$-Lys co-assemblies is determined by that of microvortices (Figure 1). Through analysis of sign and magnitude of supramolecular chirality in different outlets, the presence of racemic or enantiopure Lys is detected.

For controlled co-assembly of achiral $TPPS_4$ monomers and Lys, the laminar chiral microvortices were generated within the opposite inclined microchambers of a microfluidic device (Figure S1), while a predominantly *P* or *M* chirality of microvortices in the left (L) or right (R) microchambers was verified in previous studies (Figure S2).[11] The mixture of $TPPS_4$ (20 μM) and racemic Lys (an equimolar mixture of L-Lys and D-Lys, 5 μM) was injected into the two side inlet channels (Inlet 1 and 3) at the flow rate of 30 mL h^{-1} for each inlet, and the mixture of HCl (1.5 M) and ionic stabilizer C_2mim^+ (0.4 M) was injected through the middle inlet (Inlet 2) at the flow rate of 1 mL h^{-1} (Figure 1b). The acidification of mixing solutions within the microchannel led to symmetry breaking and self-assembly of $TPPS_4$ with Lys, the process of which was promoted by C_2mim^+. Because of the laminar flow characteristics of microfluidics,[12] the majority of co-assemblies experiencing *P* (or *M*) helical microvortices in the L (or R) microchambers were inclined to flow out through the L (or R) outlet after 100 ms (Figure S3 and Supporting Information). After keeping the solutions undisturbed for 120 min at room temperature for the growth of $TPPS_4$-Lys co-assemblies, the appearance of J-aggregates through π–π stacking of $TPPS_4$ was observed by an absorption peak at 491 nm in ultraviolet–visible (UV–Vis) spectra for solutions collected from both the L and R outlets (Figure 2a). Moreover, the enantiomorphic microvortices resulted in almost mirror CD spectra of co-assemblies from the L and R outlets, showing a negative and positive bisignate Cotton effect centered at 491.5 ± 1.0 nm (Figure 2b). The kinetics of co-assembly process of $TPPS_4$ and racemic Lys was monitored by atomic force microscopy (AFM) (Figure 2c). A gradual increase in length of supramolecular co-assemblies from 1.0 to 2.5 μm was observed in a time period of 120 min (Figure 2d). In comparison, the length of $TPPS_4$ aggregates in the absence of racemic Lys increased from 0.8 to 1.8 μm, which was shorter than that of $TPPS_4$-Lys co-assemblies. Remarkably, the intensity of CD signals ($\Delta CD = CD_{493.5 \pm 1.0\ nm} - CD_{489.5 \pm 1.0\ nm}$) in $TPPS_4$-Lys co-assemblies increased with time, suggesting a positive correlation between the size and chirality of co-assemblies (Figure S4).

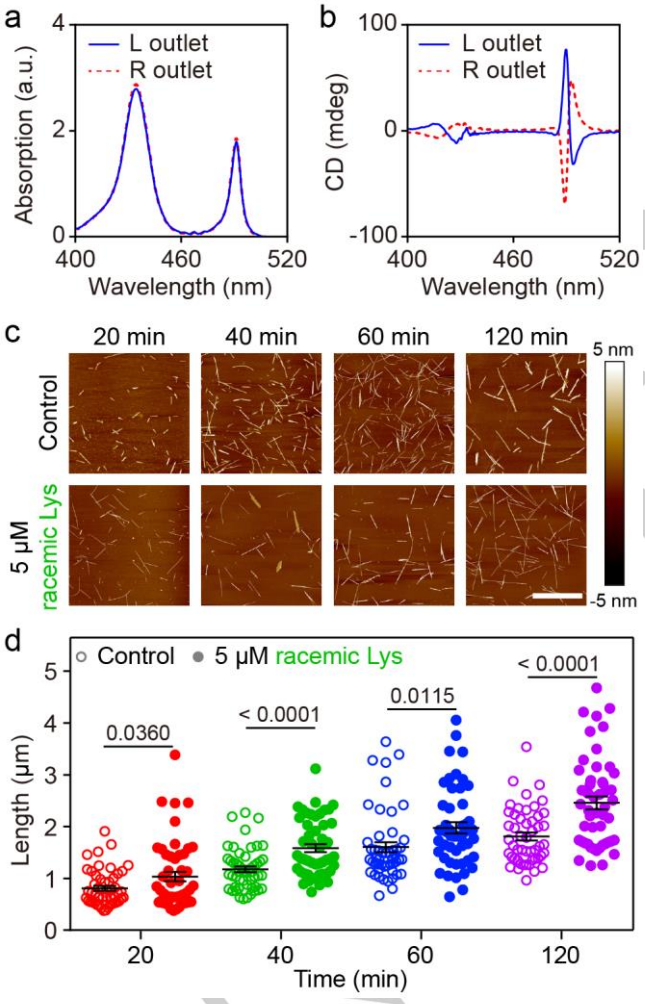

Figure 2. Characterization of supramolecular co-assemblies formed by $TPPS_4$ and racemic Lys (5 μM). (a) UV–Vis spectra and (b) CD spectra of supramolecular co-assemblies from the L (solid blue line) and the R outlet (dashed red line). (c, d) AFM analysis of growth kinetics of supramolecular co-assemblies (solid circle) and $TPPS_4$ aggregates (empty circle) up to 120 min. Scale bar, 4 μm. $n = 50$, mean ± s.e.m.

Next we investigated if it was possible to detect racemic Lys of different concentrations by this enantiomorphic microvortex-induced $TPPS_4$-Lys supramolecular system. The mixture of $TPPS_4$ (20 μM) and racemic Lys (an equimolar mixture of L-Lys and D-Lys, 0–30 μM) were injected into the side inlets (Inlet 1 and 3) of the microfluidic platform. After microvortex-controlled assembly and hierarchical growth, a negative and positive Cotton effect for $TPPS_4$-Lys co-assemblies from the L and R outlets were observed in the CD spectra (Figure S5-8). A linear response of the CD signal versus the concentration of racemic Lys from 0 to 30 μM was found for $TPPS_4$-Lys co-assemblies in both the L and R outlets (Figure 3c). The combination of sign and magnitude of ΔCD clearly indicated the presence and concentration of racemic Lys.

To illustrate the crucial role of enantiomorphic microvortex in detecting racemic Lys, alike experiments using 20 μM of $TPPS_4$ and 10 μM of racemic Lys were performed in microchambers with rectangular cross-section (Figure S9). In this case, the microvortices displayed no predominant chirality due to the symmetry in chamber geometry (Figure S9a). In the absence of any chiral polarization, the $TPPS_4$-Lys co-assemblies randomly showed either a positive or negative CD signals from the L and R outlets, which cannot be used to detect the presence of racemic Lys (Figure S9b,c). In contrast, the co-assembly of $TPPS_4$ with 10 μM L-Lys or D-Lys resulted in the same chiral sign in both outlets, indicated by a negative CD signal for $TPPS_4$-L-Lys aggregates, and a positive CD signal for

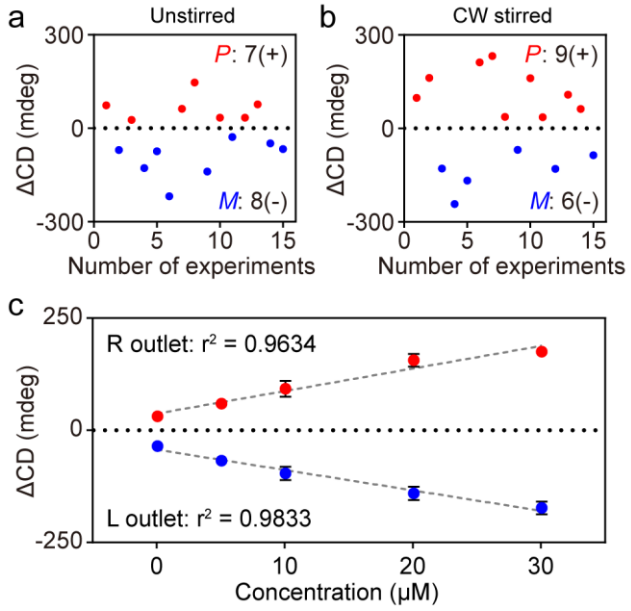

Figure 3. Detection of racemic Lys by the enantiomorphic microvortex-induced $TPPS_4$-Lys supramolecular system. CD signals of $TPPS_4$-Lys co-assemblies under (a) static and (b) CW stirring conditions. (c) CD signals of enantiomorphic microvortex-induced $TPPS_4$-Lys co-assemblies from the L and R outlets versus the concentration of racemic Lys from 0 to 30 μM (n = 3, mean ± s.e.m.).

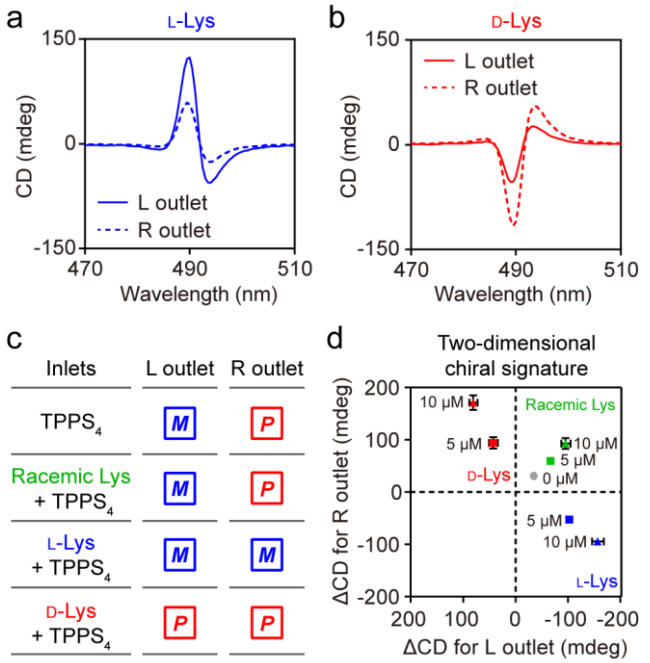

Figure 4. Differentiation of enantiopure or racemic Lys by the supramolecular system assembled in enantiomorphic microvortices. (a) CD signals of $TPPS_4$-L-Lys co-assemblies from the L and R outlets. (b) CD signals of $TPPS_4$-D-Lys co-assemblies from the L and R outlets. (c) Supramolecular chirality obtained from different outlets in the presence of enantiopure or racemic Lys. (d) Two-dimensional chiral signature of $TPPS_4$-Lys co-assemblies against the L and R outlets in the quadrant to differentiate L-Lys (L-/R-), D-Lys (L+/R+), and racemic Lys (L-/R+) (n = 3, mean ± s.e.m.).

$TPPS_4$-D-Lys aggregates (Figure S9d,e). Moreover, we performed the co-assembly of $TPPS_4$ and racemic Lys in cuvettes under static and clockwise (CW) stirring conditions (see Supporting Information for experimental details). 15 independent experiments showed 7 positive CD signals and 8 negative CD signals for $TPPS_4$-Lys co-assemblies under static conditions (Figure 3a), while 9 positive CD signals and 6 negative CD signals were observed under CW stirring conditions (Figure 3b). These CD signals with stochastic signs and magnitudes were not indicative of the presence of racemic Lys.

We next assessed the ability of supramolecular system to discriminate Lys in enantiopure form (Figure 4 and Figure S10-13). When the mixture of $TPPS_4$ (20 μM) and L-Lys (10 μM) was added into the microfluidic platform, a negative CD signal was observed in the $TPPS_4$-L-Lys co-assemblies from both the L and R outlets due to the presence of homochiral dopant L-Lys (Figure 4a and Figure S12). In addition, the higher intensity of the co-assemblies from the L outlet with respect to those from the R outlet suggested the formation of more *M* chiral aggregates in the L outlet. In contrary, the co-assembly of $TPPS_4$ (20 μM) and D-Lys (10 μM) by microfluidics resulted in a positive CD signal correlated with a predominant amount of *P* chiral aggregates in both the L and R outlets, while the R outlet displayed a higher intensity of the CD signal (Figure 4b and Figure S13). The supramolecular chirality obtained from different outlets in the presence of enantiopure or racemic Lys was summarized in Figure 4c. The two-dimensional chiral signature of $TPPS_4$-Lys co-assemblies was plotted against the L and R outlets in the quadrant, leading to the complete differentiation of L-Lys (L-/R-), D-Lys (L+/R+), and racemic Lys (L-/R+) (Figure 4d). With the increased concentration of Lys of different forms, the magnitude of CD signals was also increased.

The detection ability of enantiomorphic microvortex-induced supramolecular system was extended to identify a racemic mixture of histidine (His) (Figure S14). The mixture of $TPPS_4$ (20 μM) and racemic His (an equimolar mixture of L-His and D-His, 0–100 μM) was injected into the same microfluidic platform (see Supporting Information for experimental details). The co-assembly of $TPPS_4$ and His resulted in the formation of J-aggregates of opposite chiral signs in different outlets as characterized by CD spectra (Figure S15-18). A negative and positive CD signal corresponding to *M* and *P* chirality were observed for $TPPS_4$-His co-assemblies in the L and the R outlet, respectively. The magnitude of CD signals in both the L and R outlets increased linearly with the concentration of racemic His increasing from 0 to 100 μM (Figure S19). This behavior was similar to that of $TPPS_4$-Lys co-assemblies for detecting racemic Lys using enantiomorphic microvortices.

Unlike other supramolecular sensing systems relying on enantiomeric recognition using chiral nanostructures, our detection method applied an enantiomorphic microvortex to control over the emerging chirality of supramolecular co-assemblies of achiral $TPPS_4$ and racemic amino acids. As shown in Figure 5, the rapid mixing of $TPPS_4$, racemic Lys, and HCl in the inlet region of the microchannel resulted in the formation of two-dimensional $TPPS_4$-Lys sheet structure through

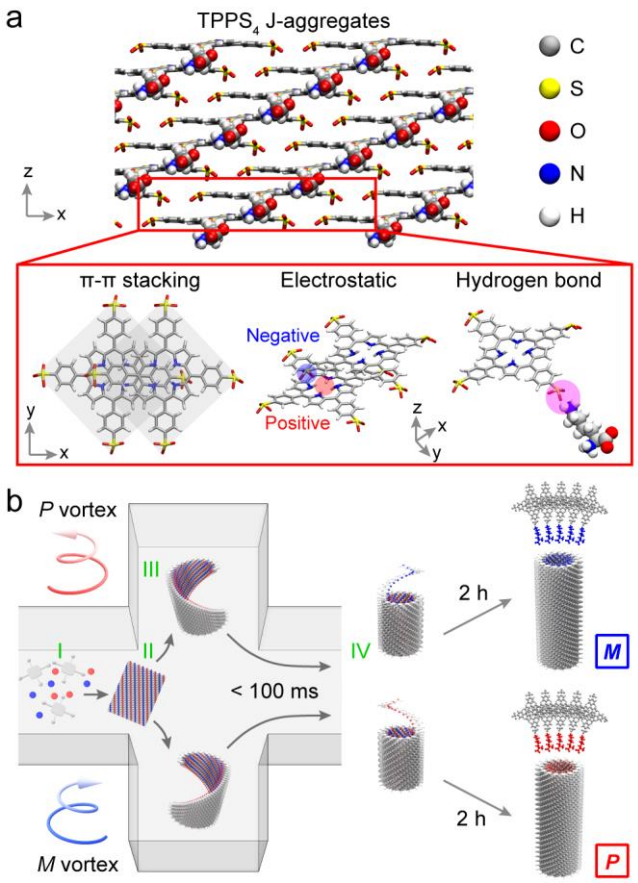

Figure 5. Illustration of enantiomorphic microvortex-enabled detection of racemic Lys. (a) Formation of two-dimensional $TPPS_4$-Lys sheet structure through the electrostatic interaction, π-π stacking, and hydrogen bonding. (b) A chiral bias toward *M* (or *P*) chirality in the *P* (or *M*) helical microvortices leading to supramolecular assembly of $TPPS_4$ and Lys of compatible chirality.

the electrostatic interaction, π-π stacking, and hydrogen bonding (Figure 5a).[13] This flexible sheet structure could be twisted by chiral microvortices inside asymmetric microchambers, as evidenced by fluid-structure interaction (FSI) simulation (Figure S20-21 and Supporting Information).[9c, 9f] Because of a sharp decrease in shear rate with the increasing chamber height, the rotation of the bottom of sheet was faster than that of the top, giving rise to a chiral bias toward *M* (or *P*) chirality in the L (or R) chamber within 100 ms (see details in Supporting Information). These chiral nuclei collected from the L and R outlets served as templates for supramolecular assembly of $TPPS_4$ and Lys of compatible chirality.[14] Note that when the amino acids coordinated to the sulfonic acid moieties of the porphyrin system, the resulting supramolecular isomers could sort themselves by aggregation (Figure S22 and Supporting Information).[15] This self-sorting effect led to the amplification of supramolecular chirality governed by the concentration of Lys (Figure 5b). For the detection of Lys in enantiopure form, the chiral nuclei with chirality preferred by the enantiomer could assemble into supramolecular systems rapidly to manifest an intense CD signal. As to the nuclei with non-preferred chirality, their growth was significantly inhibited. Subsequently, the second nucleation of $TPPS_4$-Lys yielded a weak CD signal following the chirality of enantiomer.[16] To sum up, the chiral signature of $TPPS_4$-Lys co-assemblies from different outlets was indicative of racemic and enantiomeric amino acids.

The spontaneous mirror symmetry breaking (SMSB) process of amphiphilic porphyrins goes from an achiral monomer substrate to chiral J-aggregates, leading to a stochastic distribution of chiral sign between experiments in the absence of any chiral polarization.[9b] This SMSB process is very sensitive to weak chiral polarizations,[17] so that the shear force of hydrodynamic vortexes acting at far from equilibrium conditions can converse a stochastic distribution of chiral signs between experiments in a deterministic one.[9a, 9c, 9e] SMSB selection of the chiral sign may also arise by the molecular induction exerted by the induction of a chiral molecule with the monomers and clusters at the bifurcation occurring at the formation of the critical clusters. The effect of a hydrodynamic shear force is an up-to-down effect and that of a chiral molecule is a down-to-up effect.[9f] The exploration of both effects in the microfluidic paradigm contributes to discriminative detection of racemic and enantiomeric amino acids.

In conclusion, we present an enantiomorphic microvortex-enabled supramolecular sensing system for detecting the racemic or enantiomeric form of amino acids. The initial chiral bias of $TPPS_4$-amino acid (Lys or His) sheet structure is controlled by chiral microvortices. This chiral bias toward *M* (or *P*) chirality from the L (or R) outlet leads to supramolecular assembly of $TPPS_4$ and amino acids of compatible chirality. The analysis of the sign and magnitude of supramolecular chirality in different outlets suggests the presence of racemic or enantiopure amino acids. To the best of our knowledge, this enantiomorphic microvortex-enabled sensing system may represent the first example of detecting the racemic mixture of amino acids by one-step supramolecular self-assembly without resorting to any other chiral molecules. We envision that this supramolecular sensing system with unique advantages such as straightforward operation, rapid detection, and no use of chiral additives, can find increasingly versatile applications in chiral sensing.

Experimental Section

Experimental details are provided in the Supporting Information.

Conflict of Interest

The authors declare no conflict of interest.

Acknowledgements

This work was supported financially by National Natural Science Foundation of China (21622503 and 21904028), Chinese Academy of Sciences (YJKYYQ20180055 and ZDBS-LY-SLH025), and Youth Innovation Promotion Association CAS (2016035).

Keywords: supramolecules • racemic amino acids• enantiomorphic microvortices • chirality • detection

[1] a) I. Budin, J. W. Szostak, *Ann. Rev. Biophys.* **2010**, *39*, 245-263; b) D. B. Amabilino, *Nat. Chem.* **2015**, *7*, 275; c) M. Amit, S. Yuran, E. Gazit, M. Reches, N. Ashkenasy, *Adv. Mater.* **2018**, *30*, 1707083.

[2] a) S. F. Mason, *Nature* **1984**, *311*, 19-23; b) J. L. Bada, *Nature* **1995**, *374*, 594-595; c) A. Bonetti, S. Pellegrino, P. Das, S. Yuran, R. Bucci, N. Ferri, F. Meneghetti, C. Castellano, M. Reches, M. L. Gelmi, *Org. Lett.* **2015**, *17*, 4468-4471.

[3] F. Biedermann, W. M. Nau, *Angew. Chem.-Int. Edit.* **2014**, *53*, 5694-5699.

[4] G. Pescitelli, L. Di Bari, N. Berova, *Chem. Soc. Rev.* **2011**, *40*, 4603-4625.

[5] C. Wolf, K. W. Bentley, *Chem. Soc. Rev.* **2013**, *42*, 5408-5424.

[6] a) R. Lauceri, A. Raudino, L. M. Scolaro, N. Micali, R. Purrello, *J. Am. Chem. Soc.* **2002**, *124*, 894-895; b) A. S. R. Koti, N. Periasamy, *Chem. Mater.* **2003**, *15*, 369-371; c) R. Randazzo, M. Gaeta, C. M. A. Gangemi, M. E. Fragalà, R. Purrello, A. D'Urso, *Molecules* **2019**, *24*, 84.

[7] H. Cao, X. F. Zhu, M. H. Liu, *Angew. Chem.-Int. Edit.* **2013**, *52*, 4122-4126.

[8] a) G. Storch, M. Haas, O. Trapp, *Chem.-Eur. J.* **2017**, *23*, 5414-5418; b) G. Storch, O. Trapp, *Chirality* **2018**, *30*, 1150-1160; c) K. M. Wenz, G. Leonhardt-Lutterbeck, B. Breit, *Angew. Chem.-Int. Edit.* **2018**, *57*, 5100-5104; d) W. Fang, B. Breit, *Angew. Chem.-Int. Edit.* **2018**, *57*, 14817-14821; e) J. F. Scholtes, O. Trapp, *Angew. Chem.-Int. Edit.* **2019**, *58*, 6306-6310.

[9] a) J. M. Ribó, J. Crusats, F. Sagués, J. Claret, R. Rubires, *Science* **2001**, *292*, 2063-2066; b) R. Rubires, J. A. Farrera, J. M. Ribo, *Chem.-Eur. J.* **2001**, *7*, 436-446; c) C. Escudero, J. Crusats, I. Díez-Pérez, Z. El-Hachemi, J. M. Ribó, *Angew. Chem.-Int. Edit.* **2006**, *45*, 8032-8035; d) A. D'Urso, R. Randazzo, L. Lo Faro, R. Purrello, *Angew. Chem.-Int. Edit.* **2010**, *49*, 108-112; e) Z. El - Hachemi, T. S. Balaban, J. L. Campos, S. Cespedes, J. Crusats, C. Escudero, C. S. Kamma - Lorger, J. Llorens, M. Malfois, G. R. Mitchell, A. P. Tojeira, J. M. Ribó, *Chem.-Eur. J.* **2016**, *22*, 9740-9749; f) J. M. Ribo, Z. El - Hachemi, O. Arteaga, A. Canillas, J. Crusats, *Chem. Rec.* **2017**, *17*, 713-724.

[10] a) E. Mattia, S. Otto, *Nat. Nanotechnol.* **2015**, *10*, 111-119; b) D. Komáromy, M. C. A. Stuart, G. Monreal Santiago, M. Tezcan, V. V. Krasnikov, S. Otto, *J. Am. Chem. Soc.* **2017**, *139*, 6234-6241; c) B. Liu, C. G. Pappas, E. Zangrando, N. Demitri, P. J. Chmielewski, S. Otto, *J. Am. Chem. Soc.* **2019**, *141*, 1685-1689.

[11] J. Sun, Y. Li, F. Yan, C. Liu, Y. Sang, F. Tian, Q. Feng, P. Duan, L. Zhang, X. Shi, B. Ding, M. Liu, *Nat. Comm.* **2018**, *9*, 2599.

[12] a) T. Tsukahara, K. Mawatari, T. Kitamori, *Chem. Soc. Rev.* **2010**, *39*, 1000-1013; b) A. Aota, M. Nonaka, A. Hibara, T. Kitamori, *Angew. Chem.-Int. Edit.* **2007**, *46*, 878-880; c) Q. Feng, J. P. Liu, X. Y. Li, Q. H. Chen, J. S. Sun, X. H. Shi, B. Q. Ding, H. J. Yu, Y. P. Li, X. Y. Jiang, *Small* **2017**, *13*, 1603109.

[13] A. Sorrenti, R. Rodriguez-Trujillo, D. B. Amabilino, J. Puigmartí-Luis, *J. Am. Chem. Soc.* **2016**, *138*, 6920-6923.

[14] a) A. Romeo, M. A. Castriciano, I. Occhiuto, R. Zagami, R. F. Pasternack, L. M. Scolaro, *J. Am. Chem. Soc.* **2014**, *136*, 40-43; b) N. Micali, H. Engelkamp, P. Van Rhee, P. Christianen, L. M. Scolaro, J. Maan, *Nat. Chem.* **2012**, *4*, 201-207; c) M. F. J. Mabesoone, A. J. Markvoort, M. Banno, T. Yamaguchi, F. Helmich, Y. Naito, E. Yashima, A. R. A. Palmans, E. W. Meijer, *J. Am. Chem. Soc.* **2018**, *140*, 7810-7819.

[15] M. M. Safont-Sempere, G. Fernández, F. Würthner, *Chem. Rev.* **2011**, *111*, 5784-5814.

[16] a) A. J. Markvoort, H. M. M. ten Eikelder, P. A. J. Hilbers, T. F. A. de Greef, E. W. Meijer, *Nat. Comm.* **2011**, *2*, 509; b) P. J. M. Stals, P. A. Korevaar, M. A. J. Gillissen, T. F. A. de Greef, C. F. C. Fitié, R. P. Sijbesma, A. R. A. Palmans, E. W. Meijer, *Angew. Chem.-Int. Edit.* **2012**, *51*, 11297-11301.

[17] Z. El - Hachemi, C. Escudero, O. Arteaga, A. Canillas, J. Crusats, G. Mancini, R. Purrello, A. Sorrenti, A. D'urso, J. M. Ribo, *Chirality* **2009**, *21*, 408-412.

10.1002/anie.201913882

WILEY-VCH

Entry for the Table of Contents

COMMUNICATION

We developed an enantiomorphic microvortex-enabled supramolecular sensing system for quantitative detection of racemic or enantiomeric amino acids, with unique advantages including straightforward operation, rapid detection, and no use of chiral additives.

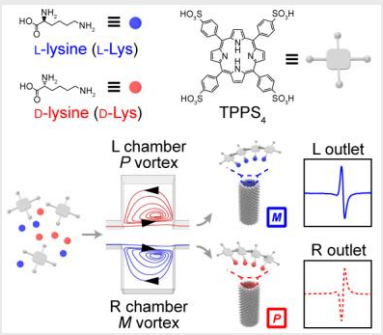

*Yike Li, Chao Liu, Xuan Bai, Fei Tian, Guoqing Hu, and Jiashu Sun**

Page No. – Page No.

Enantiomorphic Microvortex-Enabled Supramolecular Sensing of Racemic Amino Acids using Achiral Building Blocks